MECHANIKA
TEORETYCZNA
I STOSOWANA
1/2, 25, 1987

LATERAL STABILITY OF THE CANARD CONFIGURATION

TOMASZ GOETZENDORF-GRABOWSKI
ZDOBYSŁAW GORAJ

Warsaw University of Technology

1. Introduction

The Wright Brothers' aircraft was the biplane Canard. In the next years that configuration has been supplanted by conventional one. However, starting from the early part of the third decade new designs in the Canard configuration have arised. Advantages and disadvantages of that configuration have been compared and described in bibliography in respect of the performance [1, 2] but have not been published in respect of static and dynamic stability. One of few works in this field has been the analysis of an influence of the lateral flow to the dynamic stability, which has been performed by R. Panasiuk [3]. From this analysis it has followed that the lateral flow improves the stability of the phugoid and spiral modes.

In this paper dynamic equations of the small, lateral vibrations for the Canard configuration have been derived and rewritten in the dimensionless form. An influence of the some design parameters to the lateral stability has been studied. Dynamic effects resulting from a change of the low-wing configuration by a high-wing one as well as from an increase of the dihedral angle and of the fin and rudder aera and from a change of the mass balance have been analysed in detail.

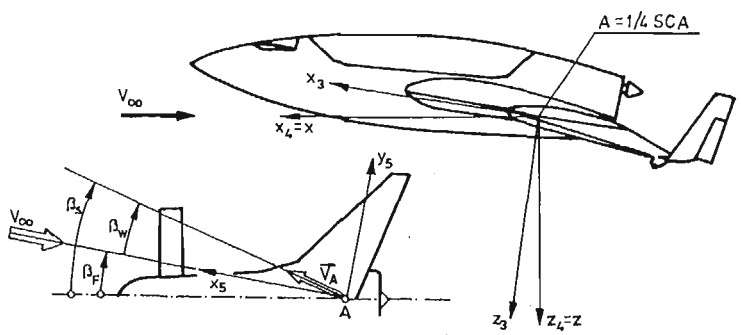

Fig. 1. System of coordinates

2. Notations

A — point denoting one-fourth of a mean aerodynamic chord (MAC)

$Axyz$ — stability axis system: x axis is directed towards the nose of fuselage, parallel to the undisturbed flow, z axis is directed downwards perpendicularly to the x axis and lies in the plane of symmetry, y axis is directed on the right wing, perpendicularly to the Axz plane (referred also as $Ax_4y_4z_4$)

$Ax_3y_3z_3$ — body axis system, obtained from $Axyz$ by the rotation α about the axis Ay

$Ax_5y_5z_5$ — flow axis system, obtained from $Axyz$ by rotation β_F about the axis Az

b — wing span

$B_{a4}(\bar{B}_{a4})$ — stiffness matrix of the anti-symmetrical model (in dimensionless form)

$\bar{b}_{a4,z}$ — dimensionless, modified, stiffness matrix of the antisymmetrical model

B_8 — stiffness matrix of the integral model

c_L — lift coefficient

g — acceleration due to gravity

J_x, J_y, J_z — moments of inertia about either stability axis system $Axyz$ or body axis system $Ax_3y_3z_3$

J_{xy}, J_{xz}, J_{yz} — products of inertia about either stability axis system $Axyz$ or body axis systen $Ax_3y_3z_3$

j_x, j_z, j_{xz} — dimensionless moments and product of inertia, respectively J_x, J_z, J_{xz}

L_v, L_p, L_r — aerodynamic derivatives of the rolling moment with respect to velocity of sideslip, rolling and yawing, respectively (either in stability axis system or body axis system)

l_v, l_p, l_r — dimensionless aerodynamic derivatives, respectively L_v, L_p, L_r

m — mass of the aircraft

M_{a4} — mass matrix of the anti-symmetrical model

$\bar{m}_{a4,z}$ — dimensionless, modified mass matrix of the antisymmetrical model

M_8 — mass matrix of the integral model

N_v, N_p, N_r — aerodynamic derivatives of yawing moment with respect to velocity of sideslip, rolling and yawing, respectively (either in stability axis system $Axyz$, or in body axis system $Ax_3y_3z_3$)

n_v, n_p, n_r — dimensionless aerodynamic derivatives, respectively N_v, N_p, N_r

p, q, r — components of a disturbance of the angular velocity either in stability axis system $Axyz$ or in body axis system $Ax_3y_3z_3$

P, Q, R — components of the angular velocity either in stability axis system $Axyz$ or in body axis system $Ax_3y_3z_3$

S — wing aera

$t, t_a, \bar{t}$ — real, aerodynamic and dimensionless time, respectively
T — period of an oscillation
$T_{1/2}$ (T_2) — time to half (to double) amplitude of an oscillation
u, v, w — components of a disturbance of the velocity either in stability axis system $Axyz$ or in body axis system $Ax_3y_3z_3$
$U, V, W(U_0, V_0, W_0)$ — coordinates of the velocity $\vec{V}_A$ (and its undisturbed components) either in stability axis system $Axyz$ or in body axis system $Ax_3y_3z_3$
$\bar{u}_0, \bar{v}_0, \bar{w}_0$ — dimensionless, undisturbed components of velocity $\vec{V}_A$ either in stability axis system $Axyz$ or in body axis system $Ax_3y_3z_3$
$\vec{V}_A$ — total velocity of the point A
x, y, z — coordinates of the mass centre in so-called design axis system. These coordinates are connected either with stability axis system $(i = 4)$ or with body axis system $(i = 3)$ by relations $x = -x_i$, $y = y_i$, $z = -z_i$
$x_8, x_{a4}, (\bar{x}_{a4})$ — small disturbance vector for integral and anti-symmetrical model (in dimensionless form), respectively
$\bar{x}_a, \bar{z}_a$ — dimensionless coordinates of the mass centre, respectively x and z
Y_v, Y_p, Y_r — aerodynamic derivatives of lateral force with respect to velocity of sideslip, rolling and yawing, respectively (either in stability axis system or in body axis system)
y_v, y_p, y_r — dimensionless aerodynamic derivatives, respectively Y_v, Y_p, Y_r
α — angle of attack
$\beta_F, \beta_W, \beta_S$ — angle of lateral flow, wind and sideslip, respectively
η — angular frequency
Θ_0 — flight-path angle
ϑ — small disturbance of the pich or flight-path angle
μ_a — dimensionless mass of the aircraft
ξ — damping coefficient
ϱ — air density
Φ_0 — bank angle
φ — small disturbance of the bank angle

3. Mathematical Model for Lateral Stability

The mathematical model, which has been used in computations, has included the mass, aerodynamic and stiffness couplings [4, 5] and will be referred as „the integral model". The linearized equations of motion have been written in matrix form [5] as follows:

$$M_8\dot{x}_8 = B_8 x_8, \tag{1}$$

where

$$\{x_8\} = \{u, v, w, p, q, r, \vartheta, \varphi\}^T \tag{2}$$

is a small disturbance vector.

Coefficients of the mass matrix M_8 and of the stiffness matrix B_8 are placed in Appendix. Physical model employed in analysis of the lateral stability has been derived from the integral model under the following assumptions:

1) steady-state trajectory can be the gliding as well as the climbing one, i.e.: $\Theta_0 \neq 0$. There can exist a sideslip: $\beta_S \neq 0$, a cross-wind: $\beta_W \neq 0$ and a lateral flow: $\beta_F \neq 0$ (where $\beta_S = \beta_F + \beta_W$)
2) there exist only anti-symmetrical disturbances from steady-state flight parameters. The small disturbance vector x_{a4} [4] has the following coordinates: v, p, r, φ. The symmetrical coordinates of the x_8 vector are equal to zero.

The anti-symmetrical model can be written as follows:

$$M_{a4}\dot{x}_{a4} = B_{a4}x_{a4}, \tag{3}$$

where matrices M_{a4} and B_{a4} can be directly derived from matrices M_8 and B_8 respectively, neglecting the uneven columns and rows. Matrices M_{a4} and B_{a4} have the form:

$$M_{a4} = \begin{bmatrix} m & mz & -mx & 0 \\ mz & J_x & -J_{xz} & 0 \\ -mx & -J_{xz} & J_z & 0 \\ 0 & 0 & 0 & 1 \end{bmatrix}, \tag{4}$$

$$B_{a4} = \begin{bmatrix} Y_v & Y_p + mW_0 & Y_r - mU_0 & mg\cos\Theta_0\cos\Phi_0 \\ L_v & L_p + m(zW_0 - yV_0) & L_r - mzU_0 & mgz\cos\Theta_0\cos\Phi_0 \\ & & & -mgy\cos\Theta_0\sin\Phi_0 \\ N_v & N_p - mxW_0 & N_r + m(xU_0 - yV_0) & -mgx\cos\Theta_0\cos\Phi_0 \\ 0 & 1 & \tan\Theta_0\cos\Phi_0 & 0 \end{bmatrix}. \tag{5}$$

Moments and products of inertia, aerodynamic derivatives and coordinates of the mass centre occuring in matrices M_{a4}, B_{a4} can be related either to the body axis system or to the stability axis system. Vectorial equation (3) expanded in the body axis system are not convenient to use in computations because in this case aerodynamic derivatives, usually known in the stability axis system $Axyz$ (or in the flow axis system $Ax_5y_5z_5$ (Fig. 2) — if the flow angle is not equal to zero) must be converted to the body axis system [5]. The same equation expanded in the stability axis system (or in the flow axis system) is more conventional because in such case we must transform only three components of the inertia pseudo-tensor and two components of the mass centre instead of the nine components of aerodynamic derivatives and two velocities (if we use the body axis system).

Numerical calculations have been performed on the basis of equations of motion in dimensionless form:

$$\bar{m}_{a4}\frac{d\bar{x}_{a4}}{d\bar{t}} = \bar{B}_{a4}\bar{x}_{a4}, \tag{6}$$

where

$\bar{t} = t/t_a$ is dimensionless time, while

$$t_a = \frac{m}{0.5\varrho V_A S} \tag{7}$$

is aerodynamic time.

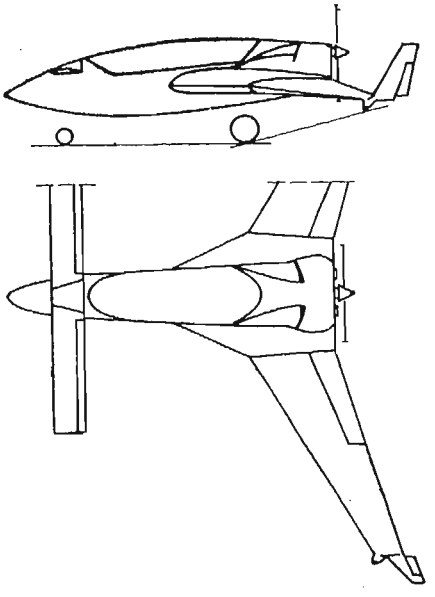

Fig. 2. Plan view of the aircraft showing the most important design parameters

One derived the following parameters:
— dimensionless mass

$$\mu_a = \frac{m}{0.5\varrho S b}, \tag{8}$$

— dimensionless coordinates of the mass centre

$$\bar{x}_a = x/b, \quad \bar{z}_a = z/b, \tag{9}$$

— dimensionless moments and products of inertia

$$j_x = \frac{J_x}{mb^2}, \quad j_z = \frac{J_z}{mb^2}, \quad j_{xz} = \frac{J_{xz}}{mb^2}, \tag{10}$$

— dimensionless velocities

$$\bar{u}_0 = \frac{U_0}{V_A}, \quad \bar{v}_0 = \frac{V_0}{V_A}, \quad \bar{w}_0 = \frac{W_0}{V_A}. \tag{11}$$

One should emphasize that in the stability axis system $\bar{u}_0 = 1$, $\bar{v}_0 = \bar{w}_0 = 0$, while in the flow axis system we have

$$\bar{u}_0 = \cos\beta_W, \quad \bar{v}_0 = \sin\beta_W, \quad \bar{w}_0 = 0. \tag{12}$$

Equation (6) has been transformed to modified form dividing its scalar components by a such coefficients in order to get the units at the main diagonal of the mass matrix. So, putting the small disturbance vector in the form

$$\bar{x}_{a4} = \left\{\frac{v}{V_A}, \frac{pb}{V_A}, \frac{rb}{V_A}, \varphi\right\} \tag{13}$$

and assuming that

1) steady-state flight is horizontal, i.e.: $\Theta_0 = 0$,

2) steady-state bank angle is equal to zero, i.e. $\Phi_0 = 0$,

3) the angles of sideslip, flow and wind are equal to zero, we can rewrite the equation of motion in the form

$$\overline{m}_{a4,z}\overset{\vee}{\overline{x}}_{a4} = b_{a4,z}\overline{x}_{a4}, \tag{14}$$

where

$$\overline{m}_{a4,z} = \begin{bmatrix} 1 & \overline{z}_a & -\overline{x}_a & 0 \\ \overline{z}_a/j_x & 1 & -j_{xz}/j_x & 0 \\ -\overline{x}_a/j_z & -j_{xz}/j_z & 1 & 0 \\ 0 & 0 & 0 & 1 \end{bmatrix}, \tag{15}$$

$$\overline{b}_{a4,z} = \begin{bmatrix} y_v & y_p & y_r-\mu_a & c_L \\ l_v/j_x & l_p/j_x & (l_r-\mu_a\overline{z}_a)/j_x & c_L\overline{z}_a/j_x \\ n_v/j_z & n_p/j_z & (n_r+\mu_a\overline{x}_a)/j_z & -c_L\overline{x}_a/j_z \\ 0 & \mu_a & 0 & 0 \end{bmatrix} \tag{16}$$

and symbol $^{\vee}$ indicates differentiating with respect to the dimensionless time.

A particular solution of the equation (14) has the form

$$\left\{\frac{v_0}{V_A}e^{\overline{\lambda}\overline{t}},\ \frac{p_0 b}{V_A}e^{\overline{\lambda}\overline{t}},\ \frac{r_0 b}{V_A}e^{\overline{\lambda}\overline{t}}\ \varphi_0 e^{\overline{\lambda}\overline{t}}\right\}. \tag{17}$$

Substitution of (17) into (14) gives the following characteristic equation

$$\det\{\overline{m}_{a4,z}\overline{\lambda}-\overline{b}_{a4,z}\} = 0, \tag{18}$$

which can be rewritten as

$$\det\begin{bmatrix} \overline{\lambda}+a & b_1\overline{\lambda}+c_1 & d_1\overline{\lambda}+e_1 & f_1 \\ h_1\overline{\lambda}+y & b_2\overline{\lambda}+c_2 & d_2\overline{\lambda}+e_2 & f_2 \\ h_2\overline{\lambda}-x & b_3\overline{\lambda}+c_3 & d_3\overline{\lambda}+e_3 & f_3 \\ 0 & -\mu_a & 0 & \overline{\lambda} \end{bmatrix} = 0, \tag{19}$$

where

$$\begin{aligned} &x = n_v/j_z, \quad y = -l_v/j_x, \quad a = -y_v, \quad b_1 = \overline{z}_a, \quad c_1 = -y_p, \\ &d_1 = -\overline{x}_a, \quad e_1 = -y_r+\mu_a, \quad f_1 = -c_L, \quad h_1 = \overline{z}_a/j_x, \\ &h_2 = -\overline{x}_a/j_z, \quad b_2 = 1, \quad c_2 = -l_p/j_x, \quad d_2 = -j_{xz}/j_x, \\ &e_2 = (-l_r+\mu_a\overline{z}_a)/j_x, \quad f_2 = -c_L\overline{z}_a/j_x, \quad b_3 = -j_{xz}/j_z, \\ &c_3 = -n_p/j_z, \quad d_3 = 1, \quad e_3 = -(n_r-\mu_a\overline{x}_a)/j_z, \quad f_3 = c_L\overline{x}_a/j_z. \end{aligned}$$

Development of (19) gives characteristic equation of order 4:

$$A\overline{\lambda}^4+B\overline{\lambda}^3+C\overline{\lambda}^2+D\overline{\lambda}+E = 0. \tag{20}$$

The coefficients of this equation can be represented as functions of x and y by the following means:

$$\begin{aligned} &A = A_0, \quad B = B_0-yB_1-xB_2, \quad C = C_0-yC_1-xC_2, \\ &D = D_0-yD_1-xD_2, \quad E = E_0-yE_1-xE_2, \end{aligned} \tag{21}$$

where

$$A_0 = r_1 - h_1 r_4 + h_2 r_7, \quad B_0 = a r_1 + r_2 - h_1 r_5 + h_2 r_8, \quad B_1 = r_4, \quad B_2 = r_7,$$
$$C_0 = d_3 f_2 - d_2 f_3 + h_1(d_1 f_3 - d_3 f_1) - h_2(d_1 f_2 - d_2 f_1) + a r_2 + r_3 - h_1 r_6 + h_2 r_9, \; C_1 = r_5,$$
$$C_2 = r_8, \quad D_0 = e_3 f_2 - e_2 f_3 - a(d_2 f_3 - d_3 f_2) + h_1(e_1 f_3 - e_3 f_1) - h_2(e_1 f_2 - e_2 f_1),$$
$$D_1 = r_6 - (d_1 f_3 - d_3 f_1)\mu_a, \quad D_2 = r_9 - (d_1 f_2 - d_2 f_1)\mu_a, \quad E_0 = -a(e_2 f_3 - e_3 f_2)\mu_a,$$
$$E_1 = (e_3 f_1 - e_1 f_3)\mu_a, \quad E_2 = (e_2 f_1 - e_1 f_2)\mu_a$$

and

$$r_1 = b_2 d_3 - b_3 d_2, \quad r_2 = c_2 d_3 - c_3 d_2 + b_2 e_3 - b_3 e_2, \quad r_3 = c_2 e_3 - c_3 e_2,$$
$$r_4 = b_1 d_3 - b_3 d_1, \quad r_5 = c_1 d_3 - c_3 d_1 + b_1 e_3 - b_3 e_1, \quad r_6 = c_1 e_3 - c_3 e_1,$$
$$r_7 = b_1 d_2 - b_2 d_1, \quad r_8 = c_1 d_2 - c_2 d_1 + b_1 e_2 - b_2 e_1, \quad r_9 = c_1 e_2 - c_2 e_1,$$

while $x = n_v/j_z$ and $y = -l_v/j_z$.

Characteristic equation in the form (20) has 4 roots, which correspond to the so-called „stiff natural modes". These modes are as follows:

— Duch Roll — an oscillatory mode possessing two predominant coordinates: the sideslip with a velocity v and the rolling with an angular velocity p. The phase-angle between these coordinates is approximately equal to 180°,

— Spiral — an unoscillatory mode possessing two predominant coordinates: the sideslip with a velocity v and the yawing with an angular velocity r, which is in phase with the sideslip,

— Rolling — an unoscillatory mode which has the one predominant coordinate, i.e.: the rolling with an angular velocity p.

4. Short Characteristic of an Aircraft Employed for Computing

The most important data are:

main wing span	$b = 7.0$ m
front wing span	$b_H = 3.6$ m
body length	$l_B = 4.5$ m
main wing aera	$S = 5.6$ m^2
front wing aera	$S_H = 1.28$ m^2
mass	$m = 470$ kg
lift-curve slope for main wing	$C^m_{L\alpha} = 4.41$ 1/rad
lift-curve slope for front wing	$C^f_{L\alpha} = 5.29$ 1/rad

The essential differences between Canard and conventional configuration, important for aircraft dynamics, are the following:

— location of a tail ahead of the wing and as a consequence decreasing of the effective angle of attack on the main wing caused by the mean downwash angle,

— location of a mass centre far ahead of the main wing, usually about 100 or more percent MAC ahead of the one fourth of MAC. For conventional configuration the mass centre is usually situated at nerby neighbourhood of the one fouth of MAC. Location

of the mass centre far ahead of the wing for Canard configuration is caused by necessity to ensure the static longitudinal tability.

As a result of the numerical computations one could get the following characteristics: angular frequency η and damping coefficient ξ, either time to half $T_{1/2}$ or time to double T_2, period T and boundaries of the stability, all for the natural modes defined before.

The following parameters were changing:

1) fin and rudder aera S_v from 0.3 m^2 to 0.7 m^2 with the steep 0.1 m^2,
2) main wing dihedral angle G from $-5°$ to $5°$ with the steep 2.5°,
3) location of the mass centre along the x axis in the body axis system, with respect to the one fourth of MAC:

$$\bar{x}_a = \frac{x_a}{b} = \{-.121, -.127, -.133\}.$$

A variation of the mass centre location was achieved by shifting forwards of a mass equal to 20 kg with the steep 1 m (it can be a baggage, accumulator, radio station etc.)

4) location of the mass centre along the z axis in the body axis system, with respect to the one fourth of MAC. There has been realized 28 values of $\bar{z}_a$ with the steep $\Delta z = 2.5$ cm (or $\Delta\bar{z}_a = 0.0036$). In reality this translocation can be achieved assuming that the mass distribution of the body is invariable but that wing-body arrangement is changeable, i.e.: that low-wing configuration can be replaced by the other one, for example by the high-wing configuration.

5. Numerical Results

At Fig. 3,4 is shown time to double amplitude of the spiral mode T_2 versus the dihedral angle G and the fin and rudder aera S_v for two different values $\bar{z}_a$. A decrease of S_v as well as an increase of G increases T_2. Comparing Fig. 3 with Fig. 4 we can notice a slight

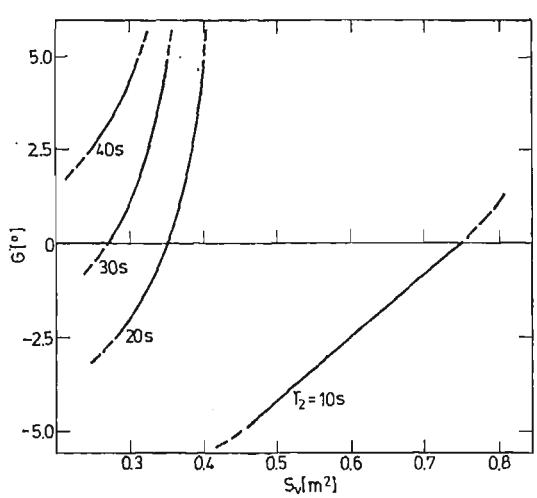

Fig. 3. Times to double amplitude T_2 of the Spiral mode as functions of S_v and G for low-wing configuration ($\bar{z}_a = 0.0159$)

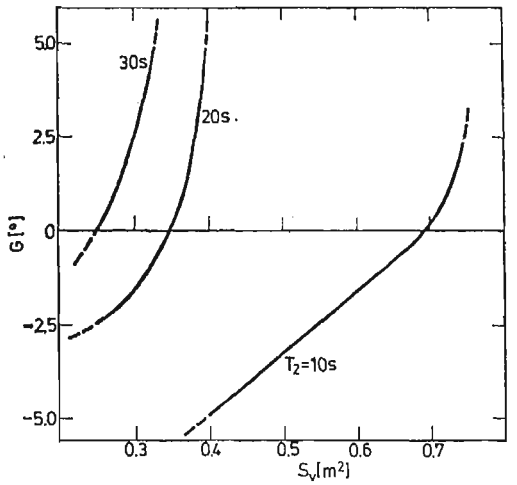

Fig. 4. Times to double amplitude T_2 of the Spiral mode as functions of S_v and G for low-wing configuration ($\bar{z}_a = 0.0279$)

increase of T_2 as $\bar{z}_a$ decreases. This dependence is shown more detail at Fig. 5, 6, from which we can read the necessary changes of S_v and G caused by variation of $\bar{z}_a$ to keep the same T_2 (T_2 is equal to 30 s and 15 s at Fig. 5 and Fig. 6, respectively). Computations show that the influence of the $\bar{x}_a$ (in the neighbourhood of $\bar{x}_a = -.127$) on the lateral dynamic stability is negligible.

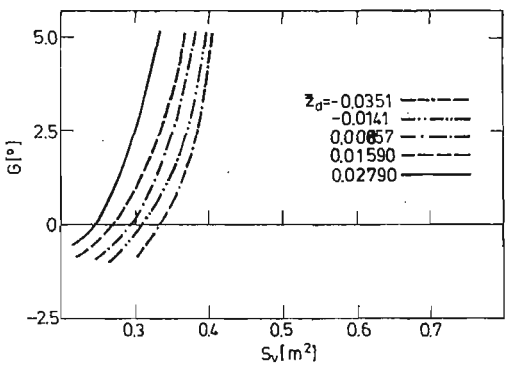

Fig. 5. Time to double amplitude T_2 of the Spiral mode (equal to 30 s) as the function of S_v, G and $\bar{z}_a$

Fig. 7-9 show the times to half amplitude $T_{1/2}$ of the Duch Roll mode as functions of G and S_v for three different values of $\bar{z}_a$. An increase of S_v as well as a decrease either of G or of $\bar{z}_a$ decreases $T_{1/2}$. An influence of S_v and G to the value $T_{1/2}$ decreases with decreasing of $\bar{z}_a$. In the case when $\bar{z}_a$ is negative $T_{1/2}$ increases as the G decreases.

Regulations FAR-23 [6] and work [4] give the definition of a boundary quotient $-\xi/\eta$ for the Duch Roll mode. This quotient must be greater or equal to 0.05. Fig. 10-12 show the value $-\xi/\eta$ as a function of G and S_v for three different values of $\bar{z}_a$. When S_v

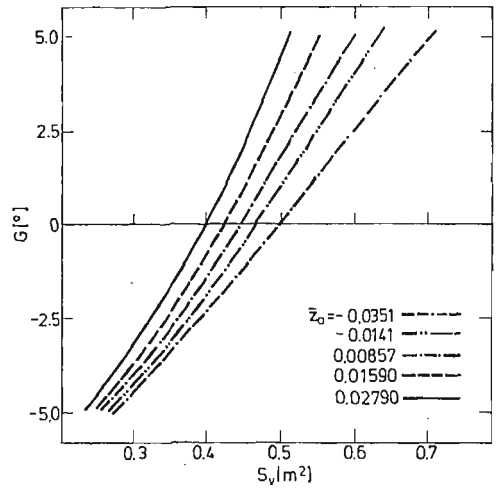

Fig. 6. Time to double amplitude T_2 of the Spiral mode (equal to 15 s) as the function of S_v, G and $\bar{z}_a$

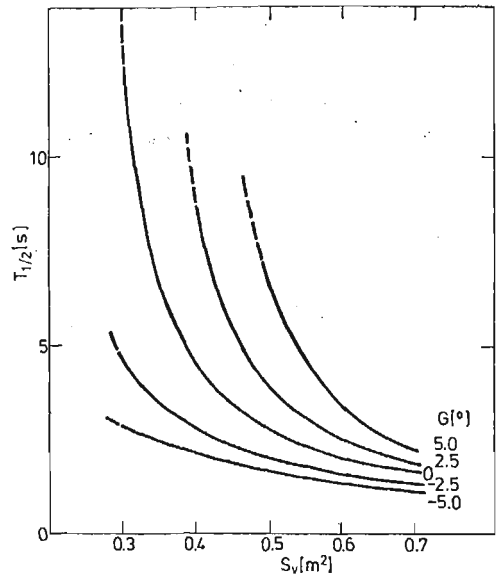

Fig. 7. Time to half amplitude $T_{1/2}$ of the Duch Roll mode as the function of S_v for different values of G in case of the low-wing ($\bar{z}_a = 0.0459$)

increases or G decreases then the quotient $-\xi/\eta$ either increases if $\bar{z}_a$ is positive or decreases if $\bar{z}_a$ is negative. An influence of S_v and G on the quotient $-\xi/\eta$ is very strong diminished in the case of negative values of $\bar{z}_a$.

Fig. 13 shows an influence of $\bar{x}_a$ to the value $T_{1/2}$ for the Duch Roll mode. Shifting to the mass centre forwards increases $T_{1/2}$. An influence of $\bar{x}_a$ to the quotient $-\xi/\eta$ is shown at Fig. 14.

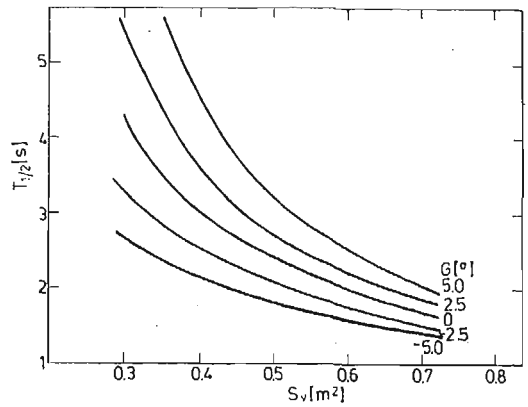

Fig. 8. Time to half amplitude $T_{1/2}$ of the Duch Roll mode as the function of S_v for different values of G in case of the low-wing ($\bar{z}_a = 0.0279$)

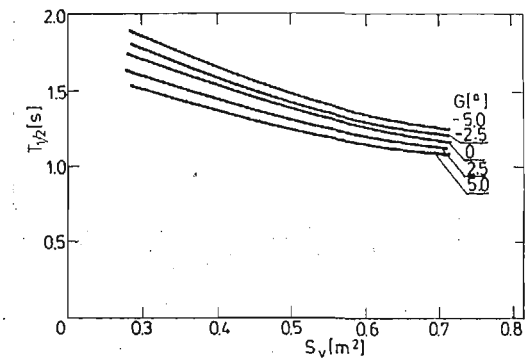

Fig. 9. Time to half amplitude $T_{1/2}$ of the Duch Roll mode as the function of S_v for different values of G in case of the mid-wing ($\bar{z}_a = 0.00857$)

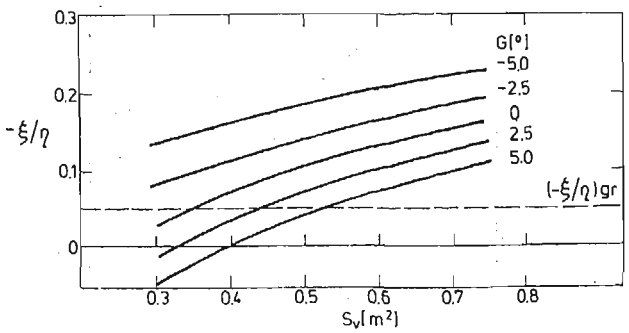

Fig. 10. Quotient $-\xi/\eta$ as the function of S_v and G in case of the low-wing ($\bar{z}_a = 0.0459$) and admissible, boundary quotient $(-\xi/\eta)_{gr}$

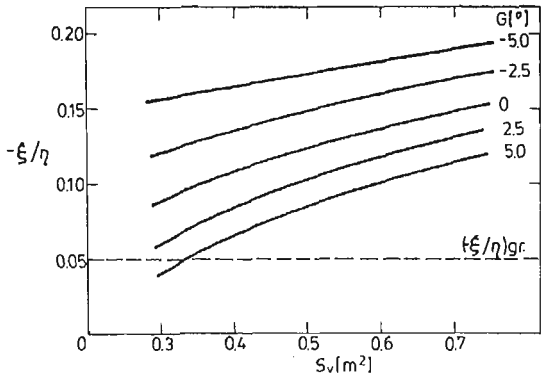

Fig. 11. Quotient $-\xi/\eta$ as the function of S_v and G in case of the low-wing ($\bar{z}_a = 0.0279$) and admissible, boundary quotient $(-\xi/\eta)_{gr}$

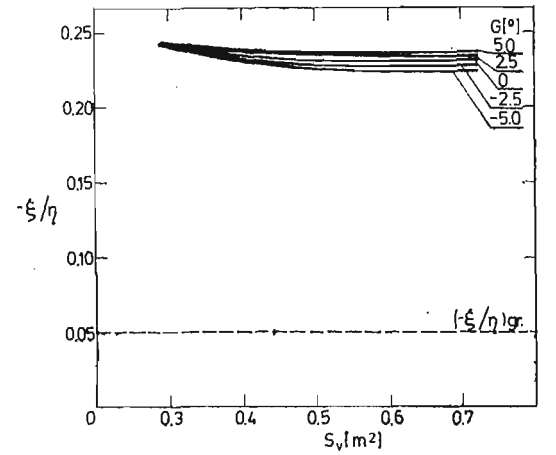

Fig. 12. Quotient $-\xi/\eta$ as the function of S_v and G in case of the mid-wing ($\bar{z}_a = 0.00857$) and admissible, boundary quotient $(-\xi/\eta)_{gr}$

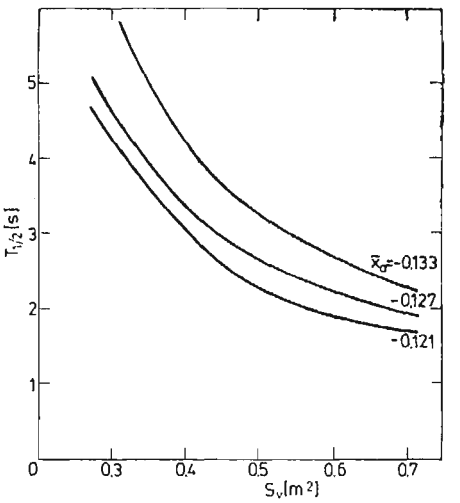

Fig. 13. Time to half amplitude $T_{1/2}$ of the Duch Roll mode as function of S_v and $\bar{x}_a$ for $G = 0°$ and $\bar{z}_a = 0.028$

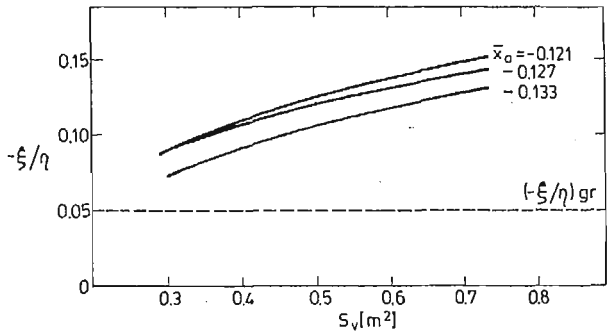

Fig. 14. Quotient $-\xi/\eta$ as the function of S_v and $\bar{x}_a$ (and admissible, boundary quotient $(-\xi/\eta)_{gr}$) for $G = 7°$ and $\bar{z}_a = 0.028$

6. Concluding Remarks

Numerical results have shown that the most important parameters for the lateral, dynamic stability of Canard configuration are: (1) vertical position of the main wing with respect to the body, (2) dihedral angle and (3) fin and rudder aera. An increase of the dihedral angle, a decrease of the fin and rudder aera as well as a shifting of the wing upwards prolong the times to double of the Spiral mode what is advantageous with point of view of the stability. Either a decrease of the dihedral angle when the fin and rudder aera is constant or an increase of the fin and rudder aera when the dihedral angle is constant can be compenseted by shifting of the main wing towards high-wing configuration.

The Duch Roll mode damping increases with an increase of the fin and rudder aera as well as with a decrease of the dihedral angle. A shifting of the mass centre forwards, improving the longitudinal static stability, deteriorates slightly the stability of the Duch Roll mode increasing the time to half amplitude of an oscillation.

7. Appendix

$$M_B = \begin{bmatrix} m & 0 & -X_{\dot{w}} & 0 & -mz & -my & 0 & 0 \\ 0 & m & -Y_{\dot{w}} & mz & 0 & -mx & 0 & 0 \\ 0 & 0 & m-Z_{\dot{w}} & my & mx & 0 & 0 & 0 \\ 0 & mz & -L_{\dot{w}}+my & J_x & -J_{xy} & -J_{xz} & 0 & 0 \\ -mz & 0 & -M_{\dot{w}}+mx & -J_{xy} & J_y & -J_{yz} & 0 & 0 \\ -my & -mx & -N_{\dot{w}} & -J_{xz} & -J_{yz} & J_z & 0 & 0 \\ 0 & 0 & 0 & 0 & 0 & 0 & 1 & 0 \\ 0 & 0 & 0 & 0 & 0 & 0 & 0 & 1 \end{bmatrix}$$

$$
\boldsymbol{B}_s = \left[\begin{array}{cccccc|cc}
X_u & X_v & X_w & X_p & X_q - mW_0 & X_r + mV_0 & -G\cos\Theta_0 & 0 \\
Y_u & Y_v & Y_w & Y_p + mW_0 & Y_q & Y_r - mU_0 & -G\sin\Theta_0\sin\Phi_0 & G\cos\Theta_0\cos\Phi_0 \\
Z_u & Z_v & Z_w & Z_p - mV_0 & Z_q + mU_0 & Z_r & -G\cos\Phi_0\sin\Theta_0 & -G\sin\Phi_0\cos\Theta_0 \\
L_u & L_v & L_w & L_p + mzW_0 - myV_0 & L_q + myU_0 & L_r - mzU_0 & -Gy\cos\Phi_0\sin\Theta_0 & -Gz\cos\Phi_0\cos\Theta_0 \\
 & & & & & & -Gz\sin\Phi_0\sin\Theta_0 & -Gy\sin\Phi_0\cos\Theta_0 \\
M_u & M_v & M_w & M_p - mxV_0 & M_q + mzW_0 + mxU_0 & M_r - mzV_0 & Gz\cos\Theta_0 & -Gx\cos\Theta_0\sin\Phi_0 \\
 & & & & & & -Gx\sin\Theta_0\cos\Phi_0 & \\
N_u & N_v & N_w & N_p - mxW_0 & N_q + myW_0 & N_r + mxU_0 - myV_0 & Gx\sin\Theta_0\sin\Phi_0 & -Gx\cos\Theta_0\cos\Phi_0 \\
 & & & & & & +Gy\cos\Theta_0 & \\
0 & 0 & 0 & 0 & \cos\Phi_0 & -\sin\Phi_0 & 0 & 0 \\
0 & 0 & 0 & 1 & \tan\Theta_0\sin\Phi_0 & \tan\Theta_0\cos\Phi_0 & 0 & 0
\end{array}\right]
$$

where $X_u, X_v, \ldots, N_q, N_r$ denote dimensional derivatives in accordance with the following definition (cited by way of example for the N_p derivative):

$$N_p = \frac{\partial N}{\partial p} = \frac{\partial(0.5\varrho V_A^2 S c_n b)}{\partial\left(\frac{pb}{V_A}\right)\frac{V_A}{b}} = \frac{\partial c_n}{\partial\left(\frac{pb}{V_A}\right)} 0.5\varrho V_A S b^2.$$

References

1. J. STASZEK, *Kaczka a samolot konwencjonalny*, TLiA, 10, Wydawnictwo Czasopism i książek Technicznych SIGMA, Warszawa 1974.
2. J. STASZEK, *Niektóre problemy układu kaczka*, TLiA, 7, Wydawnictwo Czasopism i Książek Technolicznych SIGMA, Warszawa 1980, pp. 8—13.
3. R. PANASIUK, *Dynamic Stability of Canard Configuration Including Lateral Flow*, M. Sc. Thesis (Unpublished), Warsaw University of Technology, Warszawa 1985.
4. Z. GORAJ, *Obliczenia sterowności, równowagi i stateczności samolotu w zakresie poddźwiękowym*, Preskrypt published by Zakłady Graficzne Politechniki Warszawskiej, Warszawa 1984.
5. Z. GORAJ, *Numeryczne i organizacyjne aspekty obliczeń stateczności samolotu*, Mech. Teor. Stos. 4, PWN, Warszawa 1985.
6. FAR-23, Vol. III, part 23. Federal Aviation Administration, Washington 1965 (with Amendments of 23.10.1972)

Резюме

БОКОВАЯ УСТОЙЧИВОСТЬ САМОЛЁТА ТИПА „УТКИ"

В работе представлено математическую модель малых, боковых колебаний самолета типа УТКИ. Уравнения движения записано в скоростной системе координат связаной с 1/4 середней аеродинамической хорды и доведено к безразмерному виду. Проанализировано собственные значения и формы жёстких колебаний самолёта. Представлено алгоритм вычисления пределов устойчивости двох основных форм колебаний: спирали и голландского шага. Обсуждено основные разности при исследованиях устойчивости классического самолёта и самолёта типа „УТКИ". Исследовано влияние различных геометрических конфигураций самолёта на устойчивость.

Streszczenie

STATECZNOŚĆ BOCZNA SAMOLOTU W UKŁADZIE KACZKA

Przedstawiono model matematyczny małych drgań bocznych samolotu w układzie kaczka. Równania ruchu zapisano w opływowym układzie współrzędnych związanym z 1/4 średniej cięciwy aerodynamicznej i doprowadzono do postaci bezwymiarowej. Przeanalizowano wartości własne i postacie drgań sztywnych samolotu. Przedstawiono algorytm na obliczanie granic stateczności spiralnej i stateczności holendrowania. Omówiono zasadnicze różnice przy badaniu stateczności układu klasycznego i układu kaczka. Zbadano wpływ różnych konfiguracji geometrycznych samolotu na stateczność.

Praca wpłynęła do Redakcji dnia 18 marca 1986 roku.